Preparation and Layer-by-Layer Self-Assembly of Silver Nanoparticles Capped by Graphite Oxide Nanosheets

Thierry Cassagneau and Janos H. Fendler*

Center for Advanced Materials Processing, Clarkson University, P.O. Box 5814, Potsdam, New York 13699-5814

Received: December 9, 1998; In Final Form: January 25, 1999

Sodium borohydride reduction of silver ions in aqueous dispersions of exfoliated graphite oxide (GO) resulted in the formation of remarkably monodisperse 100 Å diameter oblate Ag particles that are effectively protected by 5 Å thick GO sheets, Ag−GO. Ag−GO could be self-assembled onto poly(diallyldimethylammonium) chloride, PDDA, coated substrate; subsequent layer-by-layer self-assembly of Ag−GO and PDDA led to well-ordered ultrathin films of S-(PDDA/Ag−GO)$_n$.

Introduction

Recent burgeoning activities in the encapsulation of metallic and ferromagnetic nanoparticles by robust, yet ultrathin, graphite shells have been prompted by the potential applications of these materials in memory storage and biomedicine.[1,2] The graphite shell is produced by the Krätschmer−Huffman graphite-arc method[3] or tungsten-arc process[4] electrochemically with a molten pool of the desired metal as the anode. Alternatively, cosputtering the desired metal and graphite led to the production of thin films consisting of Co, Cu, and Ag nanocrystallites encapsulated in graphitic carbon cages.[5] As part of our overall interest in nanoparticles and nanoparticulate films we have launched a new approach for the preparation of graphite oxide encapsulated silver nanoparticles (Ag−GO) by the reduction of silver ions *in situ* in aqueous dispersions of exfoliated graphite oxide (GO). We selected GO since it is known to have ionizable carboxyl groups and charge densities as high as 1 negative charge per 30−50 Å^2.[6] Carboxylic moieties (in citrate ions[7] and poly(acrylic) acid,[8] for example) have been used for complexing the silver cations and stabilizing the metallic particles (Au and Ag, for example) formed. Furthermore, if the GO nanoplatelets are small and thin enough for undergoing a cooperative deformation, they may be able to wrap around the incipient silver nanoparticles.

Here we report the preparation and characterization of remarkably monodisperse 100 Å diameter oblate Ag particles that are effectively protected by 5 Å thick graphite oxide sheets. We also report the layer-by-layer self-assembly of ultrathin films composed of polyelectrolytes and Ag−GO nanoparticles.

Experimental Section

Materials. Silver perchlorate monohydrate (99.999%, Aldrich), poly(diallyldimethylammonium) chloride (20 wt %, PDDA, Aldrich), graphite powder (1−2 nm diameter, Aldrich), sodium chlorate (99+%, Aldrich), and poly(styrene-4-sulfonic acid) sodium salt (20% solution in water, PSS, Aldrich), sodium borohydride (98%, Sigma), and nitric acid (15.8 N, Fisher) were used as received. All aqueous solutions were prepared from 18 Ω cm water obtained by passing distilled water through a Millipore Milli-Q membrane filtration system.

Instruments. Fourier transfer infrared spectra of GO powders were recorded on a Mattson Instruments Model 2020 Galaxy Series FTIR and absorption spectra were taken on a Hewlett-Packard 8252A instrument. Atomic force microscopic (AFM) images were taken on a Topometrix Explorer 2000 scanning probe microscope in noncontact mode with standard silicon nitride tips (force constant of 0.12 N/m). A JEOL JEM-1200EXII electron microscope, operating at 120 kV, was used to characterize nanoplatelets and nanoparticles. Cyclic voltammetry was performed in aqueous 0.1 M $NH_4^+Cl^-$ deoxygenated (stream of Ar) media by a potentiostat (EG&G Princeton Applied Research, Model 273, interfaced with a computer running with the Head Start software) in a standard three-electrode electrochemical cell. The working electrode consisted of the ultrathin films self-assembled onto antimony tin oxide coated glass substrates (Delta technologies Ltd., ATO). The circuit was completed by a calomel reference electrode and a platinum auxiliary electrode.

Results and Discussion

Preparation and Characterization of the Graphite Oxide Capped Silver Nanoparticles. Colloidal dispersions of graphite oxide were prepared and characterized as previously described.[6] Briefly, the desired amount of graphite was exposed to the oxidizing mixture (HNO_3:$NaClO_3$ = 0.95:080, v/w) for 30 h at 80 °C. Elemental analysis (Galbraith Laboratories Inc.) of the resulting graphite oxide (GO) powder resulted in C = 70.43%, H = 1.56%, O = 25.05% (calculated for 57% graphite oxidation, *i.e.*, for $C_{14}H_4O_4$: C = 71.20%, H = 1.83%, O = 27.12%). The GO powders were exfoliated into GO sheets in an aqueous saline solution.[6a]

Graphite oxide capped silver nanoparticles, Ag−GO, were prepared by the reduction of silver ions *in situ* in exfoliated GO dispersions. Typically, an excess of $AgClO_4$ was added to the GO dispersion (in ratios of $[Ag^+]$:$[COO^-]$ = 10 where the concentration of carboxylate ions on GO were determined by titration), the volume was made up to 200 mL, and the pH was adjusted to 10.5 (by NaOH). Subsequent addition of 200 mL of the reducing solution (0.6 mM $NaBH_4$) was performed under vigorous stirring at room temperature. The excess metallic silver formed and the incompletely stabilized Ag and GO colloids were separated from the colloidal dispersion by filtration. The final pH of the colloidal dispersion was 9.4.

10.1021/jp984690t CCC: $18.00
Published on Web 02/25/1999

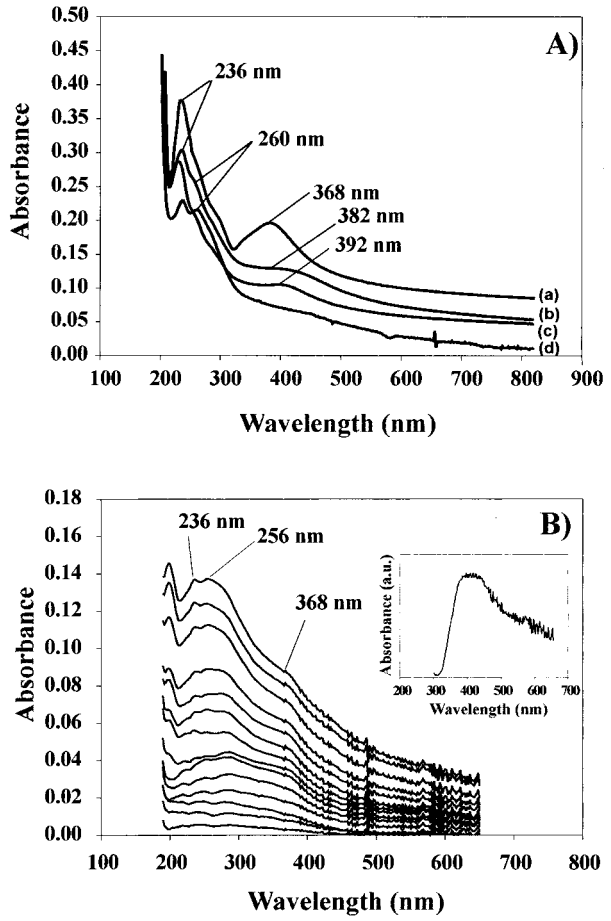

Figure 1. (A) Absorption spectra of a Ag−GO in aqueous dispersions: freshly prepared (a); after aging for 2 weeks (b), 1 month (c), and 2.5 months (d) at pH = 10. (B) Absorption spectra taken after the self-assembly of a sandwich unit of PDDA/Ag−GO on a quartz substrate. The inset shows the silver plasmon band in the S-(PDDA/Ag−GO)$_{12}$ obtained by subtracting the contribution of GO and reduced GO.

The adsorption spectrum of a freshly prepared aqueous Ag−GO dispersion is characterized by a band at 236 nm, due to GO, a shoulder at 260 nm, due to reduced GO, and a band at 368 nm due to the silver plasmon absorption (a in Figure 1A). The Ag−GO dispersion remained stable for several weeks, although the shoulder at 260 nm developed into an absorption band at the expense of the 236 and 368 nm bands, the latter of which underwent a bathochromic shift (from 368 to 392 nm, see spectra b, c, and d in Figure 1A). In fact, the absorbance ratios of GO (at 236 nm) to Ag (at 368 nm) were found to increase linearly with time (not shown). These changes are caused by the excess reducing agent, still present in the colloidal dispersion, which has the ability to partially reduce GO and hence destabilize the silver colloids. A similar behavior was observed in the absorption spectra of a PDDA/GO multilayer upon treatment by a reducing agent (hydrazine or borohydride).[9] Decreasing the pH of the aqueous Ag−GO dispersion to 5.3 led to protonation of the carboxylate groups on GO (pK_a = 6.5 for GO prepared here) and, consequently, to the decrease of the electrostatic interactions (between GO and Ag) to such an extent that flocculation occurred within a few hours. Not unexpectedly, raising the pH of the flocculated dispersion to 10 did not result in the reappearance of the silver plasmon band. These observations are in accord with the formation of GO sheet capped Ag nanoparticles (referred to as Ag−GO).

A blank experiment was performed by synthesizing Ag nanoparticles by the $NaBH_4$ reduction of silver ions *in the absence of GO* under conditions identical to those used for the preparation of Ag−GO (*vide supra*). The freshly prepared (within the first hour) silver dispersion exhibited a broad (380−600 nm) band with an intensity of *ca.* 12 times weaker than that observed for Ag−GO. Aging has further decreased the intensity of this absorption and attempts to stabilize the Ag nanoclusters by a subsequent addition of colloidal GO failed. These observations indicate the effectiveness of the stabilization of the silver surface plasmon spectra by the GO capping of Ag nanoparticles.

Additionally, for comparison (see below), silver particles were also prepared by the citrate method[7] and silver particles were also stabilized by poly(acrylic acid), Ag−PAA[8] (*in contrast to Ag−GO*).

Cyclic voltammograms of dispersed Ag−GO particles showed an almost reversible redox wave between 0 and −2 V (*vs* SCE) with an average midpoint of −1.1 V (Figure 2a−c) and the complete absence of cathodic and anodic waves between 0 and +1.0 V (Figure 2f). In contrast, cyclic voltammograms of citrate ion stabilized silver nanoparticle dispersions clearly showed the cathodic and anodic waves (with a midpoint of +0.5 V) corresponding to the reversible oxidation of silver atoms (Figure 2g).[10] Similarly, cyclic voltammograms of silver nanoparticles stabilized by poly(acrylic acid) (PAA), Ag−PAA,[8] exhibited redox waves (not shown) due to the reversible oxidation of silver atoms. Cyclic voltammetry has provided, therefore, unambiguous evidence for the effective shielding of silver nanoparticles by the encapsulation with GO. In contrast, stabilizing by PAA or citrate could not prevent silver nanoparticles from dissolution.

Morphology of the Ag−GO Nanoparticles. Aqueous dispersions of GO-capped Ag nanoparticles were transferred to a carbon-coated copper grid. Transmission electron microscopy (TEM) indicated the diameters of the Ag−GO nanoparticles to be around 100 Å, with a remarkable narrow size distribution (Figure 3). Additionally, a few large nanoplatelets (in the hundred nanometer range), due to GO, have also been visualized in some of the TEM images (not shown). Importantly, it should be remembered that TEM of colloidal dispersions of exfoliated GO (in the absence of any other particles or additives!) shows the predominant presence of circularly shaped 200−1000 Å diameter platelets in a broad size distribution along with a few larger (150−320 nm) species.[6] These sizes of the GO sheets corresponded nicely to that required for the complete encapsulation of spherical 100 Å diameter Ag nanoparticles. Indeed, taking into account the amount of GO (optically determined) and the size of silver nanoparticles (100 Å, as deduced from TEM), leads to a morphology in which each Ag nanoparticle should be capped by a 3.7 ± 0.3 Å thick GO shell. A closer inspection of the Ag−GO revealed them mainly to be oblate with an apparent continuous GO shell with a thickness of about 5 Å around the Ag particle with the exception at both poles (see Figure 3), which remained uncovered. This uncovered area accounted for 15−16% of the total surface of the Ag−GO particle and is likely to have a high negative charge density owing to the presence of borohydride ions and/or other anions formed in the reduction step. If we take into account the effective coverage of the Ag particles (85%), we estimate an average thickness of 4.25 Å for the GO shell, a value very close to that deduced by optical absorption. It should be noted that the GO capsule did not tightly adhere to the silver core. This suggests the incomplete reduction of silver ions during the encapsulation

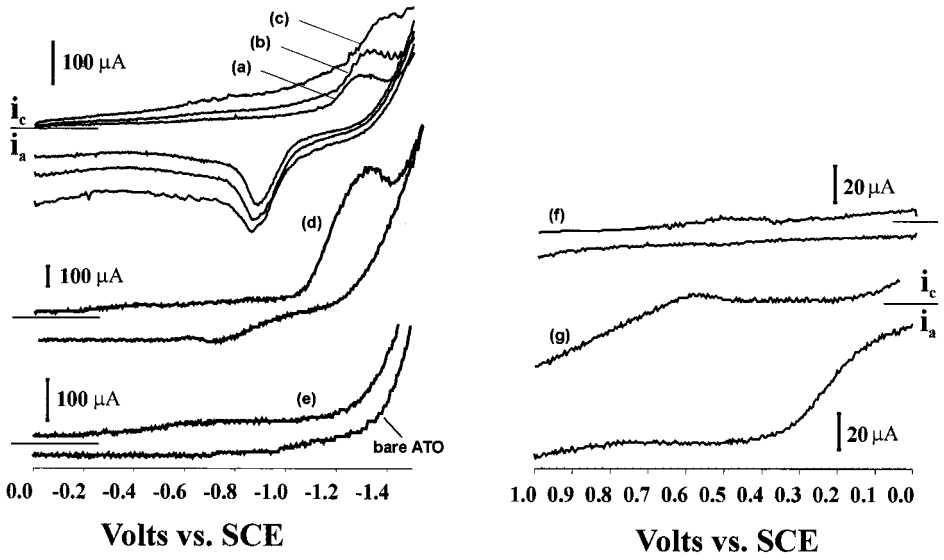

Figure 2. Cyclic voltammograms of aqueous Ag−GO dispersions at 100 mV/s (a), 200 mV/s (b), and 400 mV/s (c) sweep rates. Also shown is the cyclic voltammogram of an ATO-(PDDA/Ag−GO)$_4$ film (d) and the bare ATO (e) in a 0.1 M $NH_4^+Cl^-$ electrolytic medium at a scan rate of 100 mV/s. Cyclic voltammograms obtained by scanning an ATO electrode between 0 and +1 V *vs* SCE for the same aqueous Ag−GO dispersion (f) and for an aqueous Ag nanoparticle dispersion, prepared by the citrate method (g) are also given. Both (f) and (g) were recorded at a scan rate of 100 mV/s.

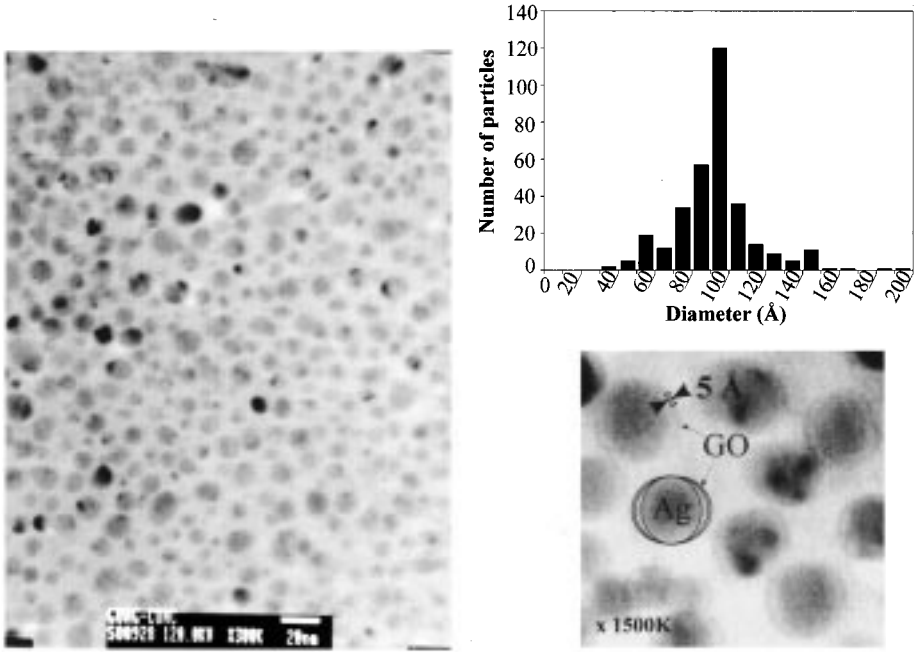

Figure 3. Transmission electron microscopy (TEM) image of Ag−GO nanoparticles.

by GO. Subsequent reduction leads then to a shrinkage of the volume the Ag nanoparticles occupy.

Layer-by-Layer Self-Assembly. Ag−GO nanoparticles were self-assembled onto well-cleaned (2 min immersion into H_2SO_4:H_2O_2 = 75:25, v/v, followed by copious washing with deionized water) ATO-coated glass slides or quartz substrates. A positively charged primer layer (20 Å thick), was first deposited onto these substrates by immersion into an aqueous 10^{-3} M PDDA solution (pH = 6.5) for 4 min, followed by thorough rinsing with deionized water and drying by N_2. Immersion of the primed substrate into an Ag−GO dispersion for 30 min, followed by thorough rinsing with deionized water and drying by N_2 resulted in the formation of a self-assembled S-(PDDA/Ag−GO)$_n$ film.

Self-assembly of Ag−GO nanoparticles was attempted onto both positively (S-PDDA) and negatively (S-PDDA/PSS) charged substrates by the established methodology.[11] The Ag−GO nanoparticles self-assembled only onto the positively charged PDDA substrate, providing evidence for the presence of negative charges on the outer surface of the Ag−GO nanoparticles. Self-assembled S-(PDDA/Ag−GO)$_n$ films, consisting of *n* number of sandwich units, were formed by the alternating immersions of the substrate into aqueous PDDA solution (4 min) and into freshly prepared aqueous Ag−GO dispersion (30 min) for *n* number of times and the rinsing by water and the drying by N_2 between the adsorption of each PDDA and Ag−GO layer.

AFM images of S-(PDDA/Ag−GO) indicated a good substrate coverage and an average value of the peak-to-valley distance of 70 Å (Figure 4). Apparently, cationic PDDA reorganized itself around the Ag−GO particles. Self-assembly of a subsequent layer of PDDA (to form an S-(PDDA/Ag−

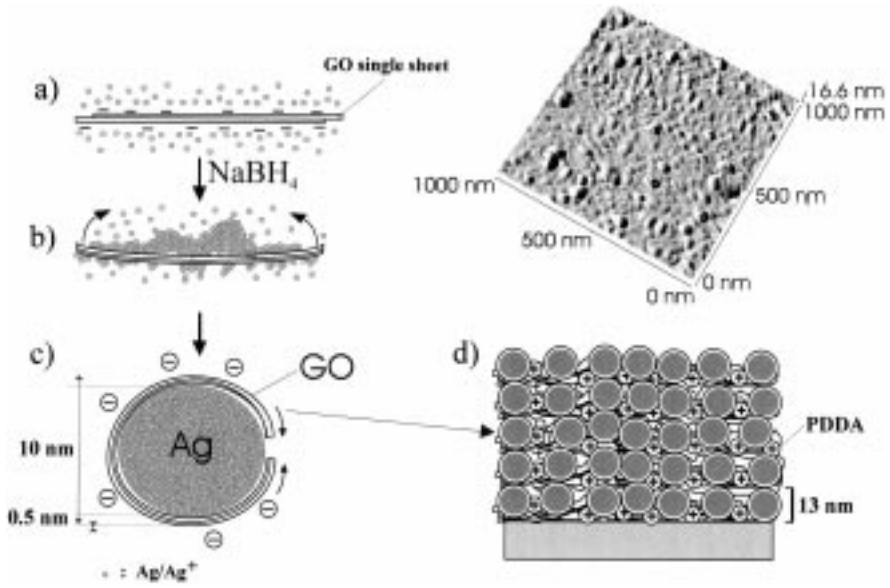

Figure 4. Schematics of Ag−GO formation mechanism: adsorption of silver cations onto the GO nanosheets (a), followed by a reductive treatment to form Ag cluster preferentially on the concave surface of GO sheets (b) and by the wrapping of the GO around the Ag clusters to form Ag−GO (c). The layer-by-layer assembly of PDDA and Ag−GO nanoparticles onto a given substrate leads to highly organized arrays (d) with high density of surface coverage, as illustrated by the AFM image.

GO/PDDA) film) resulted in a very flat topology (RMS value = 3.5 Å) with an average peak-to-valley height of 13 Å only.

Absorption spectra of the self-assembled S-(PDDA/Ag−GO)$_n$ films are characterized by bands with absorption maxima at 236 nm (due to GO) and at 256 nm (due to reduced GO) and a shoulder at 368 nm characteristic of the silver plasmon absorption (see Figure 1B). The self-assembly was monitored by absorption spectrophotometry, which indicated the regularity of the layer-by-layer growth (Figure 1B). A simple calculation, taking into account the amount of GO (optically determined) relative to the size of silver nanoparticles (an average diameter of 100 Å, as deduced from TEM) laid down in a close-packed array onto a polycation layer (as shown by AFM, Figure 4), indicates that each nanoparticle is protected by a 3.7 ± 0.3 Å thick shell of GO. Taking $\epsilon_{368nm} = 1.25 \times 10^4$ M^{-1} cm^{-1} for the plasmon absorption band of silver nanoparticles[12] and having an absorption increment of 6.42×10^{-3} at 368 nm for each Ag−GO/PDDA sandwich layer deposited, one can estimate that the volume of silver present per square cm of bilayer is 5.2×10^{-13} m^3. This is in a remarkably good agreement with the value of 5.5×10^{-13} m^3, obtained by considering a close-packed array of 100 Å Ag particles capped with a 5 Å thick GO shell. It should be noted that the absorbance ratio (measured after deconvolution of the bands) of GO (at 236 nm) to reduced GO (at 356 nm) in a self-assembled S-(Ag−GO/PDDA)$_{12}$ film was found to be significantly smaller (0.6) than that in the aqueous Ag−GO dispersion (2.4). This observation is interpreted to imply the preferential self-assembly of Ag−GO nanoparticles over GO sheets onto PDDA.

The stabilizing effect of GO was also demonstrated by the examination of films self-assembled from naked silver nanoparticles (i.e., Ag particles prepared under the same conditions as used for Ag−GO but without GO) and PDDA. In contrast to the films self-assembled from GO-protected Ag (*i.e.*, S-(PDDA/Ag−GO)$_n$), AFM imaging of S-(PDDA/Ag) revealed the presence of very small particles with an average peak-to-valley distance of 8 Å (with extreme values ranging from 4 to 20 Å, not shown), and the absorption spectrum manifested itself in two plasmon absorption bands of equal intensity (centered

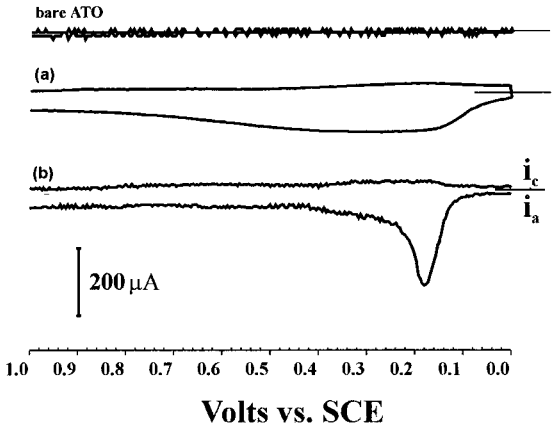

Figure 5. Cyclic voltammograms of ATO-(PDDA/Ag−GO)$_4$ (a) and ATO-(PDDA/Ag-PAA)$_4$ (b) films at a scan rate of 100 mV/s in a 0.1 M $NH_4^+Cl^-$ solution. Both anodic waves are characteristic of silver oxidation.

at 294 and 340 nm), indicating the presence of nonmetallic silver clusters and small metallic nanoparticles (below 30 Å), respectively.[13]

Stabilities of S-(PDDA/Ag−GO)$_4$ and S-(PDDA/Ag-PAA)$_4$ films were also investigated by cyclic voltammetry in a spectroelectrochemical cell in which the self-assembled films (S = ATO) served as the working electrode (Figure 5). Cycling the S-(PDDA/Ag−GO)$_4$ film between −2 and 0 V showed the presence of an irreversible reduction wave at a potential of −1.3 V (*vs* SCE) at the first scan, confirming the incomplete reduction of GO. Similar observation was previously reported for S-(PDDA/GO)$_n$ films.[9] Cycling the ATO-(PDDA/Ag−GO)$_4$ film at positive potential, a broad anodic wave (centered at +0.29 V *vs* SCE) was observed during the two first cycles (Figure 5a), indicative of an irreversible oxidation of metallic silver. Concomitantly, we also noticed a 20 nm oscillation of the Ag plasmon absorption band after each cycling of the potential from 0 to 2 V or 0 to −2 V. This was due to the electrical polarization of the film, the cathodic polarization displacing the plasmon absorption band to shorter wavelengths while absorption at longer wavelengths was the consequence of an incomplete

reduction of silver cations.[14] The irreversible oxidation wave of metallic silver observed in the two first scans at positive potential accounted for 3×10^{-4} Cb per deposited layer involving only 5.3×10^{-4}% of the total silver amount. It should be noted that the molar amount of silver relative to GO was nearly 3500 times higher. This implies that silver particles were effectively stabilized by the GO thin shell since the dissolution of only 5.3×10^{-4}% of the silver particles occurred in the self-assembled multilayers. This is likely to have originated in the incompletely stabilized silver domains. For comparison, cycling the S-(Ag-PAA/PDDA)$_4$ film between -2 and $+2$ V always showed an irreversible oxidation wave of the same amplitude (observed for at least 15 consecutive cycling), $+0.18$ V (*vs* SCE, Figure 5b), demonstrating significant silver dissolution (6.5×10^{-3}% of the silver particles after 15 cycles) and hence inefficient protection of the Ag particles from dissolution. It should be noted that a layer of Ag−PAA covered the substrate only about half as densely as Ag−GO, as evidenced by AFM and optical absorption.

Mechanism of Ag−GO Formation. Experimental evidence and simple calculations have been marshaled for formation of Ag−GO (*i.e.*, 100 Å diameter spherical Ag nanoparticles encapsulated by 4−6 Å diameter GO sheets) in the *in situ* reduction of silver ions in GO dispersions. The mechanism for Ag−GO formation involves at least four steps: (i) the reduction of silver cations on the surface of GO sheets, (ii) nucleation of small silver clusters at different sites, (iii) growth of the silver clusters, and (iv) bending of the GO sheets around the Ag particles. Although each of these steps are reasonable, we can only speculate on their relative time scale. A feasible mechanism may be governed by the dissymmetrical distribution of silver cations on the apposing GO surfaces. This would facilitate the flexing and bending of the very thin GO sheets, the faster rate of nucleation, and the preferential formation of silver clusters on the concave surface. Cluster growth would then lead to spherical Ag nanoparticles localized on the concave sides of GO sheets. Ample evidence has been obtained for the *in situ* formation of spherical nanoparticles from cations initially evenly distributed on layer surfaces.[15,16] The correct size and thickness of the GO sheets are believed to be responsible for the ultimate wrapping of the Ag nanoparticle (Figure 4). The observed narrow size distribution of the Ag−GO nanoparticles (Figure 3) is in accord with this hypothesis. Too large GO sheets would favor uneven aggregation and ultimate precipitation, while a too thick GO sheet would not be flexible enough for bending and encapsulating the Ag particles.

Concluding Remarks

Preparation of Ag−GO nanoparticles, reported here, opens the door, in principle, to the construction of any spherical metallic nanoparticles within an ultrathin shell whose resistivity can be controlled by the extent of its oxidation. Furthermore, the monodispersed metallic core ultrathin shell composite nanoparticles prepared are amenable to the formation of well-ordered two-dimensional arrays and three-dimensional networks that may find potential applications as advanced electronic or electro-optical devices and could function as high-density rechargeable batteries by intercalating and deintercalating lithium ions. Exploration of these and related projects are under active investigation in our laboratories.

Acknowledgment. Support of this work by the New York State Science and Technology Foundation and Clarkson University's Center for Advanced Materials Processing (CAMP) is gratefully acknowledged.

References and Notes

(1) (a) Ruoff, R. S.; Lorents, D. C.; Chan, B.; Malhotra, R.; Subramoney, S. *Science* **1993**, *259*, 346. (b) Tomita, M.; Saito, Y.; Hayashi, T. *Jpn. J. Appl. Phys.* **1993**, *32*, L280. (c) Seraphin, S.; Zhou, D.; Jiao, J. *J. Appl. Phys.* **1996**, *80*, 2097. (d) Saito, Y.; Nishikubo, K.; Kawabata, K.; Matsumoto, T. *J. Appl. Phys.* **1996**, *80*, 3062. (e) Elliott, B. R.; Host, J. J.; Dravid, V. P.; Teng, M. H.; Hwang, J.-H. *J. Mater. Res.* **1997**, *12*, 3328.

(2) (a) Host, J. J.; Block, J. A.; Parvin, K.; Dravid, V. P.; Alpers, J. L.; Sezen, T.; LaDuca, R. *J. Appl. Phys.* **1998**, *83*, 793. (b) Block, J. A.; Parvin, K.; Alpers, J. L.; Sezen, T.; Laduca, R.; Host, J. J.; Dravid, V. P. *IEEE Transactions on Magnetics*; IEEE-Inst. Electrical Electronics Engineers Inc.: New York, 1998; pp 982−984.

(3) Krätschmer, W.; Lamb, L. D.; Fostiropoulos, K.; Huffman, D. R. *Nature* **1990**, *347*, 354.

(4) (a) Dravid, V. P.; Host, J. J.; Teng, M. H.; Elliott, B. R.; Hwang, J.-H.; Johnson, D. L.; Mason, T. O.; Weertman, J. R. *Nature* **1995**, *374*, 602. (b) Teng, M. H.; Host, J. J.; Hwang, J.-H.; Elliott, B. R.; Weertman, J. R.; Mason, T. O.; Dravid, V. P.; Johnson, D. L. *J. Mater. Res.* **1995**, *10*, 233. (c) Host, J. J.; Teng, M. H.; Elliott, B. R.; Hwang, J.-H.; Mason, T. O.; Weertman, J. R.; Johnson, D. L.; Dravid, V. P. *J. Mater. Res.* **1997**, *12*, 1268.

(5) (a) Hayashi, T.; Hirono, S.; Tomita, M.; Umemura, S. *Nature* **1996**, *381*, 772. (b) Babonneau, D.; Cabioc'h, T.; Naudon, A.; Girard, J. C.; Denanot, M. F. *Surf. Sci.* **1998**, *409*, 358.

(6) (a) Cassagneau, T.; Fendler, J. H. *Adv. Mater.* **1998**, *10*, 877. (b) Cassagneau, T.; Fendler, J. H. Manuscript in preparation.

(7) (a) Carey-Lea, M. *Am. J. Sci.* **1889**, *37*, 476. (b) Siiman, O.; Bumm, L. A.; Callaghan, R.; Blatchford, C. G.; Kerker, M. *J. Phys. Chem.* **1983**, *87*, 1014.

(8) Ung, T.; Giersig, M.; Dunstan, D.; Mulvaney, P. *Langmuir* **1997**, *13*, 1773.

(9) Kotov, N. A.; Dékány, I.; Fendler, J. H. *Adv. Mater.* **1996**, *8*, 63.

(10) The silver oxidation potential is cited to be $+0.56$ (*vs* SCE) in the *Handbook of Chemistry and Physics*, 64th ed.; (CRC Press, Inc.: Boca Raton, FL).

(11) (a) Decher, G.; In *Templating, Self-Assembly and Self-Organization*; Sauvage, J.-P.; Hosseini, M. W., Eds.; Comprehensive Supramolecular Chemistry, Vol. 9; Pergamon Press: Oxford, U.K., 1996; pp 507−528. (b) Schmitt, J.; Decher, G.; Dressick, W. J.; Brandow, S. L.; Geer, R. E.; Shashidhar, R.; Calvert, J. M. *Adv. Mater.* **1997**, *9*, 61.

(12) Mulvaney, P. In *Electrochemistry in Colloids and Dispersions*; Mackay, R. A., Texter, J., Eds.; VCH: New York, 1992; Chapter 26, p 347.

(13) (a) Henglein, A. *Chem. Rev.* **1989**, *89*, 1861. (b) Henglein, A.; Linnert, T.; Mulvaney, P. *Ber. Bunsen-Ges. Phys. Chem.* **1990**, *94*, 1449. (c) Henglein, A. *Isr. J. Chem.* **1993**, *33*, 77.

(14) Mulvaney, P. *Langmuir* **1996**, *12*, 788.

(15) (a) Malla, P. B.; Komarneni, S. *Mater. Res. Soc. Symp. Proc.* **1993**, *286*, 323. (b) Kiraly, Z.; Dékány, I.; Mastalir, A.; Bartok, M. *J. Catalysis* **1996**, *161*, 401. (c) Burkett, S. L.; Press, A.; Mann, S. *Chem. Mater.* **1997**, *9*, 1071.

(16) (a) Rabenberg, L. K.; Nunn, C. M.; Mallouk, T. E. *Chem. Mater.* **1991**, *3*, 149. (b) Kotov, N. A.; Putyera, K.; Fendler, J. H.; Tombacz, E.; Dékány, I. *Colloids and Surfaces A-Physicochemical and Engineering Aspects* **1993**, *71*, 317. (c) Cassagneau, T.; Hix, G. B.; Jones, D. J.; Maireles-Torres, P.; Rhomari, M.; Rozière, J. *J. Mater. Chem.* **1994**, *4*, 189. (d) Dékány, I.; Fendler, J. H. In *Fine Particles Science and Technology - From Micro to Nanoparticles*; Pelizzetti, E., Ed.; NATO Advanced Science Institute Series; Kluwer: Dordrecht, The Netherlands, 1996; pp 443−455.